Available online at www.sciencedirect.com

ScienceDirect

Procedia CIRP 102 (2021) 399–404

www.elsevier.com/locate/procedia

18th CIRP Conference on Modeling of Machining Operations

Parameterization method for non-linear friction models of machine tool feed drives

Michael Wiesauer*, Friedrich Bleicher

Institute of Production Engineering and Photonic Technologies, TU Wien, Getreidemarkt 9, 1060 Vienna, Austria

* Corresponding author. Tel.: +43-1-58801-311382; fax: +43-1-58801-931101. *E-mail address:* wiesauer@ift.at

Abstract

During machining operations, there are permanent interactions between the digital servo control and the machine structure. In addition to the mass and stiffness properties, different damping effects in the system take influence on the feed drive dynamics. Virtual prototypes of machine tools allow the investigation as well as the characterization of damping in single feed axes. In this paper, the friction mechanisms in the drive train are investigated by using the example of a three-axes milling machine. Dynamic friction models are parameterized and coupled with a mechatronic simulation model of the machine tool. Adequate parameterization of nonlinear friction models further increases the accuracy of the machine tool model in motion simulation.

Keywords: Modeling; Friction; Positioning; Machine tool

1. Introduction

Machine tools are dynamically excited through the internal forces of the machining process and through external reaction forces due to transient motion. The latter are caused by the setpoint, the controller parameterization and the non-linearity of the frictional forces, and are related to the interactions between the feed drives and the machine structure. Thus, machine tool feed drives determine the quality of the components to be machined and the productivity of the value adding processes with their positioning accuracy and speed. Modeling of the kinematic and dynamic behavior coupled with a model of the drive control enables the investigation and improvement of machine tools already in the design process [1,2].

Regarding the deviation between the reference and actual position during feed motions, a distinction is made between the error inside the servo loop and the error outside the servo loop [3]. Depending on the geometry and the kinematic structure of the machine tool, these errors differ to a larger or minor extent. This fact and the required accuracy determine the choice of the structural mechanics modeling method. Ansoategui et al. [4] described the modeling of the dynamic behavior of a test rig using a three degrees of freedom (DOF) lumped mass model. Sato et al. [5] used the rigid multibody simulation to analyze the motion trajectories of a machining center with semi-closed control loop. This allows the bodies to be connected with discrete spring-damper systems, but the elasticities of the bodies themselves are not taken into account. Flexible multibody simulation, in contrast, supports the integration of finite element (FE) models and large movements on flexible structures [6]. The Craig-Bampton theory [7] is used in flexible multibody as well as finite element simulations to reduce the number of degrees of freedom of individual bodies and to increase the efficiency [8]. In comparison, with modal superposition, the finite element model of the entire machine is order-reduced via modal analysis. Furthermore, the structural behavior is linearized in the modeled axis state and, in contrast to the flexible multibody simulation, allows only small guiding movements [9]. Lee et al. [10] used this method to predict surface quality with a coupled simulation of a vertical machining center incorporating a cutting force model.

10.1016/j.procir.2021.09.068

Especially during trajectories where the direction of motion is changed, the frictional forces acting in the feed drive mechanism take influence on the deviations between the reference and actual position. There is a variety of static and dynamic models for the mathematical description of friction, which differ in terms of accuracy, number of parameters and suitability for simulation [11]. Based on these, dynamic errors can be predicted and compensated by feedforward [12,13].

This paper presents the integration of a nonlinear friction model for feed drives into a mechatronic simulation model of a machine tool. The friction model is parameterized based on the kinematic behavior and measurements of the torque-generating actual current value during various interpolation movements. Thus, the prediction accuracy of the dynamic error in the transient simulation is increased and an assessment of the dynamics in velocity reversals is enabled.

2. Mechatronic machine tool model

The simulation and investigation of the dynamic error under consideration of friction was carried out on a test machining center of the company Fill GmbH. In this type of machine, the horizontally arranged main spindle and thus the tool is positioned with a serial, three-axis kinematics, as shown in Fig. 1. The individual feed drives are translationally moved by a ball screw system coupled to a synchronous motor and guided by roller rail systems. The positioning of the axes is performed with a SIEMENS 840D Computer Numerical Control (CNC) system and a S120 drive system, using a linear scale for closed position control of the respective axis. Leveling mounts with vibration isolation plates attached to the machine bed form the foundation and thus the interface between the machine structure and the ground.

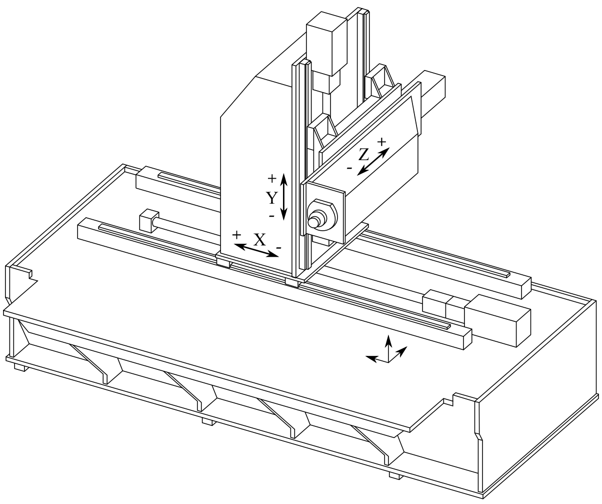

Fig. 1. Geometry and kinematics of the examined test machining center.

In the present work, a coupled simulation model, which has been validated under the effect of external dynamic forces and described in detail by [14] is used. In the following subsections, the modeling methods are briefly introduced, with special emphasis on the simulation of transient effects in positioning movements.

2.1. Mechanical model

In order to achieve high simulation accuracy despite the large operating strokes of the axes (X, 1770 mm; Y, 655 mm; and Z, 685 mm), a finite element model created in the commercial software ANSYS Workbench forms the basis of the mechatronic simulation model. Using the eigenvalues and eigenvectors determined by an undamped modal analysis, the mechanical system is transformed into a state space model suitable for digital block simulation [14]. Assuming that higher frequency modes do not significantly affect the overall system behavior, the first-order differential equation system is reduced and all modes above 1000 Hz are neglected. This increases the computational efficiency, which is very crucial for time domain simulation, with imperceptible deviations in terms of accuracy. Through the order-reduced state space model, the deformations of the machine linearized around an operating point are described. However, if singularities in the stiffness matrix are taken into account, a detection of guiding movements restricted to this axis position is possible [9]. The modeling of the kinematic and dynamic properties in the ball screw according to [14] results in a statically underdetermined system and, consequently, in rigid body modes when modal analysis is performed. These modes allow freely moveable feed drives in the respective directions. Except for the rigid body modes, the modal damping approach is assumed for the remaining modes. The mechanical model represents the controlled system and is coupled with the other components in a graphical programming environment. The block diagram of the coupled simulation model used in this work with the model of the mechanical structure, the control model and the friction model is schematically depicted in Fig. 2.

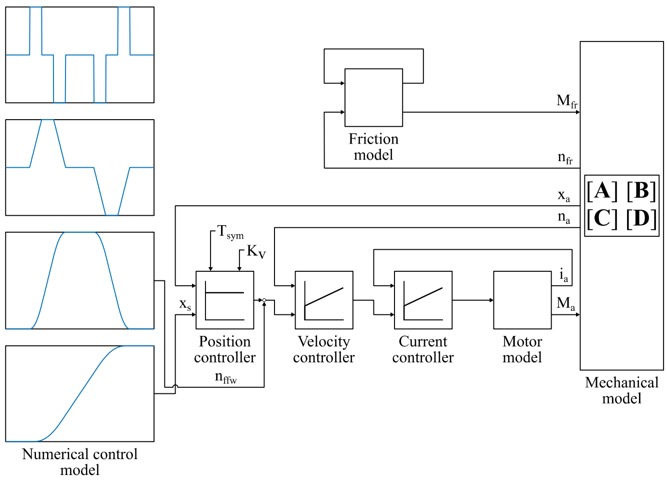

Fig. 2. Schematic representation of the mechatronic machine tool block diagram based on [14].

2.2. Control model

During the operation of machine tool feed drives, the CNC system calculates the reference variables for the subsequent controlled drives by parsing the NC code. With regard to high productivity capabilities, high path velocities and accelerations are required, but these are restricted by the physical drive and structure limits [15]. The acceleration trajectory determines with its frequency content the bandwidth of the excitation generated by the setpoint specification. By limiting the maximum jerk or by further smoothing the trajectories, the bandwidth of the excitation can be reduced [1].

To investigate the dynamic error during positioning, the setpoint values are calculated in a simplified numerical control model as presented in Fig. 2. Since single linear interpolated movements of one or more axes are sufficient to evaluate the path dynamics, the simplification is to assume that the velocity at the beginning and at the end of the trajectory are zero. The trajectories for the desired position and velocity values are calculated with the maximum jerk and acceleration values in the interpolation cycle at discrete points of time. These interpolation points are extended by a piecewise, cubic spline interpolation, whereby the setpoint values are transmitted to the control in the position control cycle.

The position and velocity setpoints (x_s and n_{ffw}) are converted into a drive torque M_a by a model of the drive control and the drive based on [14], as schematically shown in Fig. 2. In order to reduce the tracking error, the velocity reference input weighted by a feedforward factor of one is added to the position controller output. The dynamics of the individual axes are considerably increased by feedforward control and subsequently tend to overshoot with velocity changes [15]. This effect is reduced by delaying the values generated by fine interpolation with the balancing time of the symmetry filter T_{sym} before calculating the position difference (x_s−x_a) [16]. The proportional gain of the position control loop K_v is thus only effective for the disturbance response. The actual velocity n_a fed back from the state space model is used in the velocity controller with reference model to calculate the input variable for the downstream current controller [14]. A field-oriented model of the synchronous motor based on [17] completes the representation of the drive control.

2.3. Friction model

In machine tool components such as bearings, profiled rail systems and ball screws, related frictional forces and moments act in the moving directions. Rigid body modes are not oscillatory and consequently are not damped in the model by the modal approach [18]. Modeling the friction effects as external forces allows them to be taken into account and offers a high degree of flexibility with regard to the mathematical description. The LuGre model published in [19] describes the dynamic friction behavior in the position-dependent pre-sliding as well as in the velocity-dependent sliding regime using bristles. Liu et al. [20] modified the LuGre model to increase the accuracy of simulation results during the transition between sticking and sliding compared to measured values. With the so-called transmission engaging model (TEM), the frictional force is defined as:

$$F = k\sigma_0 z + \sigma_1 \frac{dz}{dt} + \sigma_2 v \tag{1}$$

where σ_0 represents the stiffness, z the deflection and σ_1 the micro viscous damping factor of an average bristle. σ_2 describes the viscous damping factor and v is the relative velocity between two surfaces. The surfaces between two bodies in contact are approximated by means of additional contact components (driven parts) [20]. During velocity reversal, the number of driven parts carried by the moving part increases. The model conception with a single contact component is shown in Fig. 3.

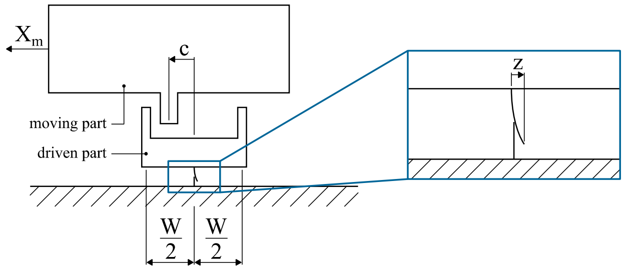

Fig. 3. Schematic representation of the TEM based on [20].

The friction force in the pre-sliding regime is scaled in Eq. 1 by the variable k, which is defined as:

$$k = \gamma + \lambda(t)\left(1-\gamma\right). \tag{2}$$

The constant γ describes the friction force at the beginning and the position-dependent variable $\lambda(t)$ during the transition section. The engaging level is defined as:

$$\lambda(t) = \begin{cases} \dfrac{W/2 + c(t)}{W} & ,if\ z \geq 0 \\ \dfrac{W/2 - c(t)}{W} & ,if\ z < 0. \end{cases} \tag{3}$$

W represents the average distance of the engaging process and is shown in Fig. 3. The position-dependent variable $c(t)$ is defined as:

$$c(t) = \begin{cases} W/2 & ,if\ c(t-T_S) + \Delta X_m(t) \geq W/2 \\ -W/2 & ,if\ c(t-T_S) + \Delta X_m(t) \geq -W/2 \\ c(t-T_S) + \Delta X_m(t) & \end{cases} \tag{4}$$

with

$$\Delta X_m(t) = X_m(t) - X_m(t-T_S), \tag{5}$$

where T_S is the sampling time and ΔX_m is the distance traveled by the moving part during this time. The friction force model is completed by the internal state equation

$$\frac{dz}{dt} = v - \frac{|v|}{g(v)} z \tag{6}$$

with $g(v)$ according to [21]:

$$g(v) = \left(F_C + \left(F_S - F_C\right)^{-\left(\frac{|v|}{v_S}\right)^{\beta}} + F_{\log} \ln\left(\frac{|v|}{v_{\log}} + 1\right)\right)\frac{1}{\sigma_0}, \tag{7}$$

where F_C is the Coulomb friction, F_S is the static friction, v_S represents the Stribeck velocity, β is the shape factor, $F_{\log}$ represents the force and $v_{\log}$ the velocity of the logarithmic part of the friction force.

In the overall model, each individual feed axis is coupled with a friction model. This calculates with the virtually measured angular velocity n_{fr} of the motor rotor the friction torque M_{fr}, which is fed back into the mechanical model as a counter-torque, as shown schematically in Fig. 2.

3. Linear model behavior

The drive torque to be applied during traversing movements is composed of an inertia and a friction part and can be measured via the drive current using the CNC internal trace function. If the inertia is represented by the model with high accuracy, it is consequently possible to draw conclusions about the proportion of friction. In general, the complex transfer behavior between a force acting on a mass with a single degree of freedom and the resulting speed are characterized by a constant decrease in magnitude of 20 dB per decade. The resulting straight line in the Bode magnitude plot depends exclusively on the mass and on the rotary inertia of the system, respectively.

Fig. 4 shows the comparison between measured and simulated frequency responses of the speed-controlled system – the ratio between motor speed and motor torque – of the X- and Z- axis. Friction was neglected in the simulation model, whereby the frequency response functions describe the linear system behavior. In the frequency range up to approximately 12 Hz, the measurements have been slightly influenced by the velocity controller and the current setpoint filters, which has led to discontinuities in this range. Apart from this, the frequency response of the speed-controlled system is determined exclusively by the mechanical structure of the machine tool. In the lower frequency range the components of the feed axes respond like a rigid system. Comparing the results of experiment and simulation, it can be inferred that the mass ratios were modeled with a sufficiently high accuracy. Furthermore, the zeros and poles of the frequency response function are predicted by the state space model.

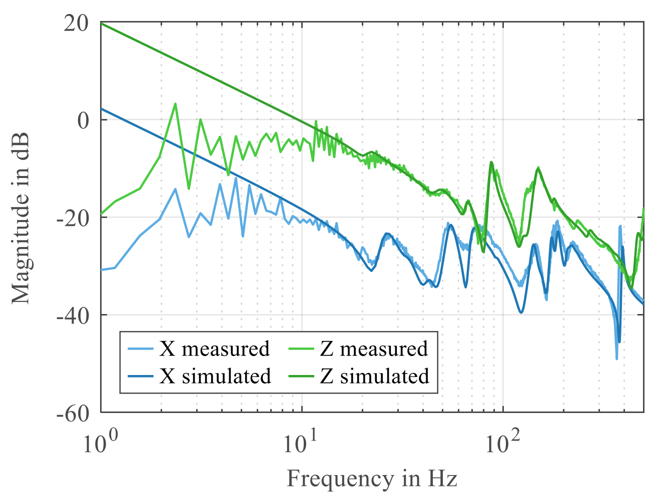

Fig. 4. Measured and simulated frequency responses of the speed-controlled system of the X- and Z-axis.

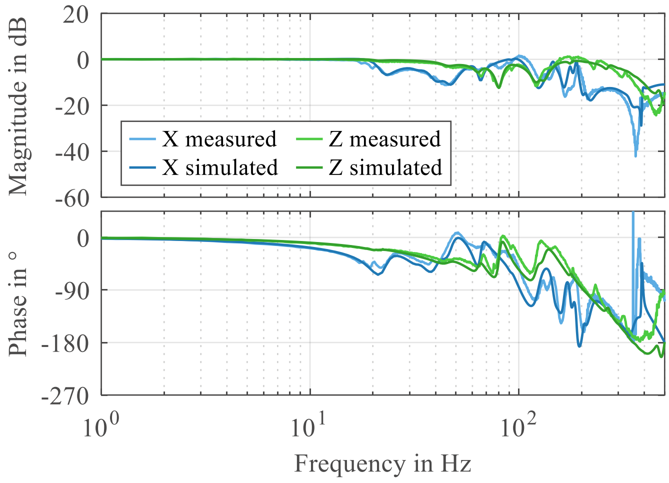

Fig. 5. Measured and simulated reference frequency responses of the velocity controller of the X- and Z-axis.

Subsequently, the state space model was coupled with the drive control model. The latter was parameterized based on the gain factors, time constants and function modules adjusted at the test machining center.

The behavior of the cascaded control loop significantly influences the deviation between the reference and actual position during motion trajectories. In order to validate the model in the frequency domain, the reference frequency response of the velocity controller – the ratio between the actual speed value and the speed setpoint of the motor – was measured experimentally. Fig. 5 depicts the Bode plot of the measured and simulated reference frequency responses of the velocity controller in the X- and Z-direction. The −3 dB bandwidth used for characterizing the speed of the controller differs by 2 Hz in the X-axis and by 3 Hz in the Z-axis. The slight deviations of the magnitude in the controlled system (see Fig. 4) consequently also effect the magnitude of the reference frequency response at approximately 100 Hz in the X-axis and at 175 Hz in the Z-axis. However, it can be concluded that the model is capable of accurately representing the behavior of the closed speed loop.

4. Model behavior during feed movements

The mechatronic model validated by the investigations in the frequency domain was subsequently used for the parameterization of the associated friction model. As already mentioned, the torque-generating actual current value is composed of an inertia and a friction part. Defined by the torque constant, the proportional relationship between the torque-generating current and the drive torque enables the calculation of the latter. At constant feed rate, the component of inertial force becomes zero. Therefore, to identify the parameters of the stationary friction force from Eq. 7, the individual axes of the test machining center were accelerated to a defined speed and the drive current was measured. The model behavior in the pre-sliding regime an in the transition region to the sliding regime is determined by the bristle stiffness σ_0, the micro viscous damping factor σ_1, and the factors W and γ of the TEM. These parameters were identified by measurements of the drive current during sinusoidal axis movements. The measurement signals were acquired with the CNC internal data logger at a sampling frequency of 500 Hz.

Fig. 6 shows the comparison between measured and simulated results during a positioning operation of the Z-axis with 5000 mm/min feed rate. The finite element model was linearized at the axis positions X 800 mm, Y 327 mm and Z 100 mm, and was coupled with the models of friction and drive control including speed feedforward. The reference trajectories were limited in the CNC system and in the model, respectively, with the maximum values of jerk (150 m/s^3) and acceleration (14.4 m/s^2). Fig. 6a shows the position controller performance and an overshoot at the end of the ramp response with an oscillation frequency of about 21 Hz in the measurement as well as in the simulation results. This natural frequency results from a tilting of the machine bed caused by the installation conditions and can also be seen in the frequency response of the speed-controlled system (Fig. 4). The influence of the leveling mounts is damped in a simplified linear approach in the model, whereas the elastomer plates installed show nonlinear behavior. This simplification has the effect of a longer settling time in the simulation results, although the dynamic error is very small, as depicted in Fig. 6a. The drive torque as a function of time shown in Fig. 6b demonstrates the influence of the friction model especially in the constant and zero velocity range. After the overshoot is damped by the micro viscous friction component, a constant counter-torque remains at zero velocity. It should be noted that due to machine's internal settings a negative actual current value is output for acceleration in the positive Z-direction (see Fig. 1).

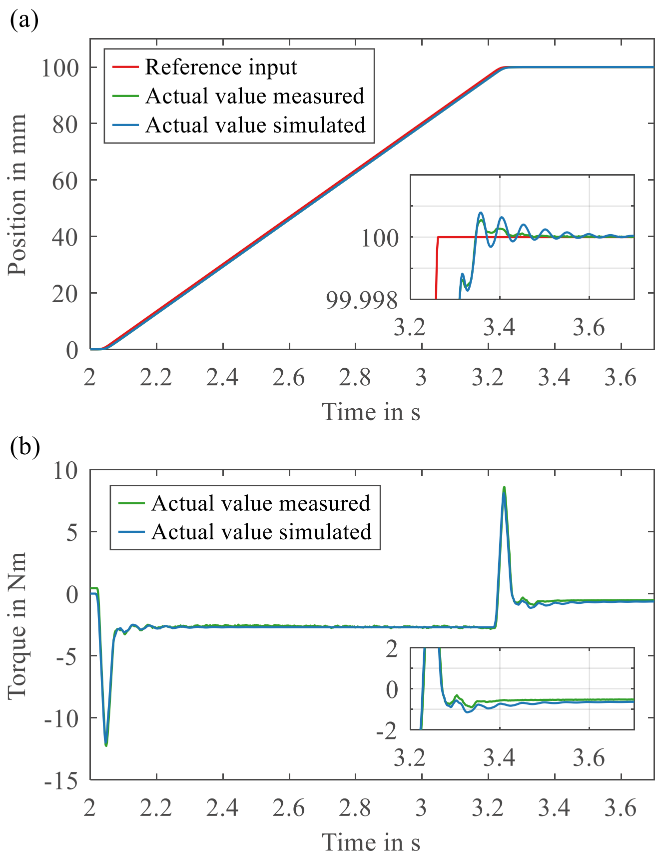

Fig. 6. Comparison of measured and simulated results for Z-axis positioning with 5000 mm/min: (a) position; (b) driving torque.

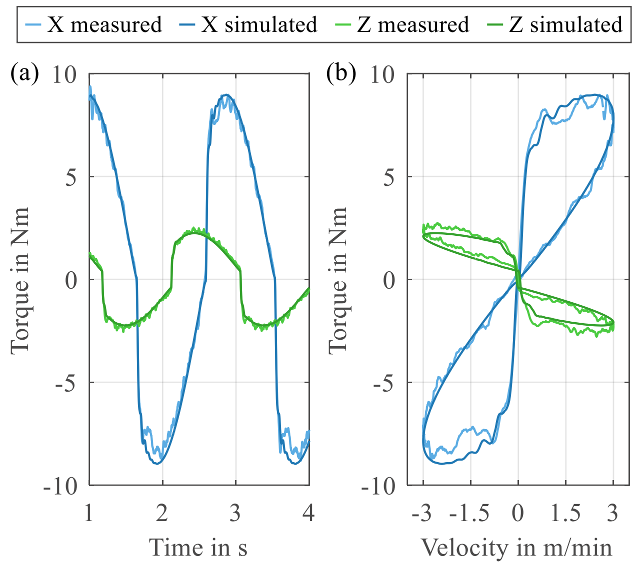

Fig. 7. Experimental and simulation results of a circular path in X-Z-plane with radius 15 mm and feed rate 3000 mm/min: (a) driving torque as a function of time and (b) as a function of velocity.

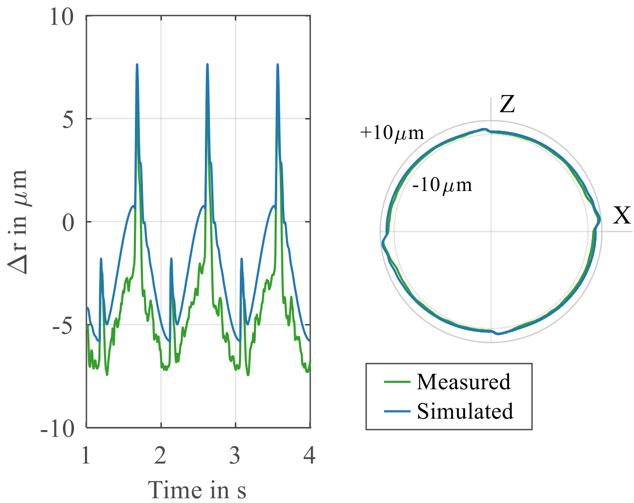

Fig. 8. Measured and simulated contour accuracy for counterclockwise circular path.

The measured and simulated driving torques of the X- and Z-axis during a circular interpolation motion (radius 15 mm, feed rate 3000 mm/min) are shown in Fig. 7. For the simulation, the reference variables measured at the machine were used as input. In Fig. 7a, the measured values show a slightly direction-dependent behavior in the X- as well as in the Z-axis, whereas the simulation model behaves ideally symmetrical. The effect of the TEM on the LuGre model at low velocity is evident in Fig. 7b. The frictional torque increases at the zero crossing with the slope determined by σ_0, which subsequently decreases in the transition region. Finally, the friction is determined by the stationary equation.

Fig. 8 shows the comparison of the contour accuracy of the circular interpolation motion measured on the linear scales of the closed position control loop. The polar plot shows the contour error scaled up by a factor of 100 and the deviations of ±10 µm from the ideal circle. The height and shape of the quadrant glitches are simulated accurately; however, a slightly larger radius results. This deviation is due to the symmetry filter mentioned in Section 2.2. The filter was parameterized in the simulation model with the balancing time set in the machine. Since the sum of the time delays of the velocity-controlled drive slightly differs (0.6 ms), a small deviation results with regard to the tracking error.

5. Conclusions

In the present contribution, the simulation accuracy of a modal reduced finite element model coupled with a drive control and a friction model during interpolation movements was investigated. The so-called transmission engaging friction model was parameterized based on the linear behavior of a three-axis test machining center and acted in the overall model as a counter-torque at the motor rotors of the feed drives.

The comparison of measured and simulated dynamic position errors revealed that the behavior during interpolation movements is very well represented by the model. In addition to linear damping, overshoot at the end of acceleration pulses is damped by the effect of the friction model. The increasing accuracy during velocity reversal by the TEM can be confirmed, reducing simulation deviations for quadrant glitches. The modeling method allows to infer the dynamics of machine tool already in the development process by virtual tests; however, the determined friction parameters are limited to similar machine components and geometries. Further experimental investigations are necessary to determine the influence of manufacturing inaccuracies and wear on the friction behavior as well as on the overall model.

Acknowledgements

The IFT of TU Wien as well as the authors want to express great appreciation and gratitude to the Machine Tool Technologies Research Foundation (MTTRF) and the company Fill GmbH for supporting the research work in the field of production engineering.

References

[1] Altintas Y, Verl A, Brecher C, Uriarte L, Pritschow G. Machine tool feed drives. CIRP Ann 2011;60:779-796.

[2] Altintas Y, Brecher C, Weck M, Witt S. Virtual Machine Tool. CIRP Ann 2005;54:115-138.

[3] Lyu D, Liu Q, Liu H, Zhao W. Dynamic error of CNC machine tools: a state-of-the-art review. Int J Adv Manuf Technol 2020;106:1869-1891.

[4] Ansoategui I, Campa FJ, López C, Díez M. Influence of the machine tool compliance on the dynamic performance of the servo drives. Int J Adv Manuf Technol 2017;90:2849-2861.

[5] Sato R, Tashiro G, Keiichi S. Analysis of the Coupled Vibration between Feed Drive Systems and Machine Tool Structure. Int J Autom Technol 2015;9:689-697.

[6] Zaeh M, Siedl D. A New Method for Simulation of Machining Performance by Integrating Finite Element and Multi-body Simulation for Machine Tools. CIRP Ann 2007;56:383-386.

[7] Craig RR, Bampton MCC. Coupling of substructures for dynamic analyses. AIAA J 1968;6:1313-1319.

[8] Law M, Phani AS, Altintas Y. Position-Dependent Multibody Dynamic Modeling of Machine Tools Based on Improved Reduced Order Models. ASME J Manuf Sci Eng 2013;135:021008.

[9] Berkemer J. Gekoppelte Simulation von Maschinendynamik und Antriebsregelung unter Verwendung linearer Finite Elemente Modelle. Ph.D. Thesis, Universität Stuttgart, Stuttgart, Germany; 2003.

[10] Lee CH, Yang MY, Oh CW, Gim TW, Ha JY. An integrated prediction model including the cutting process for virtual product development of machine tools. Int J Mach Tools Manuf 2015;90:29-43.

[11] Marques F, Flores P, Pimenta Claro JC, Lankarani HM. A survey and comparison of several friction force models for dynamic analysis of multibody mechanical systems. Nonlinear Dyn 2016;86:1407-1443.

[12] Sato R. Generation Mechanism of Quadrant Glitches and Compensation for it in Feed Drive Systems of NC Machine Tools. Int J Autom Technol 2012;6:154-162.

[13] Jamaludin Z, Van Brussel H, Swevers J. Quadrant glitch compensation using friction model-based feedforward and an inverse-model-based disturbance observer. 10th IEEE International Workshop on Advanced Motion Control, Trento, 2008, pp. 212-217.

[14] Wiesauer M, Habersohn C, Bleicher F. Validation of a Coupled Simulation for Machine Tool Dynamics Using a Linear Drive Actuator. J Manuf Mater Process 2021;5(1):1.

[15] Zirn O. Machine Tool Analysis - Modelling, Simulation and Control of Machine Tool Manipulators. Habilitation Thesis, ETH Zürich, Zurich, Szwitzerland; 2008.

[16] Groß H, Hamann J, Wiegärtner G. Elektrische Vorschubantriebe in der Automatisierungstechnik. Erlangen: Publicis MCD; 2000.

[17] Isermann R. Mechatronische Systeme - Grundlagen. 2nd ed. Berlin: Springer; 2008.

[18] Oertli ET. Strukturmechanische Berechnung und Regelungssimulation von Werkzeugmaschinen mit elektromechanischen Vorschubantrieben, Ph.D. Thesis, TU München, Munich, Germany; 2003.

[19] Canudas de Wit C, Olsson H, Åström KJ, Lischinsky P. A New Model for Control of Systems with Friction. IEEE Trans Automat Contr 1995;40:419-425.

[20] Liu CC, Tsai MS, Cheng CC. Development of a novel transmission engaging model for characterizing the friction behavior of a feed drive system. Mech Mach Theory 2019;134:425-439.

[21] Kunc M. Identifikation und Modellierung von nichtlinearen Dämpfungseffekten in Vorschubachsen für Werkzeugmaschinen, Ph.D. Thesis, RWTH Aachen, Aachen, Germany; 2013.